

ACTIVE TECTONICS IN THE ARGENTINE PRECORDILLERA AND WESTERN SIERRAS PAMPEANAS

Lionel L SIAME.¹, Olivier BELLIER¹ and Michel SEBRIER²

¹ Université Paul Cézanne (Aix-Marseille III) - CEREGE, Europôle de l'Arbois, B.P. 80, 13545 Aix-en-Provence Cedex 4, France.

² Université Pierre et Marie Curie, Laboratoire de Tectonique, 4 Place Jussieu, 75005 Paris, France.

* Corresponding author: siame@cerege.fr

ABSTRACT

The Andean foreland of western Argentina (28°S-33°S) corresponds to retroarc deformations associated with the ongoing flat subduction of the Nazca plate beneath the South American lithosphere. This region is characterized by high levels of seismic activity and crustal active faulting. To improve earthquake source identification and characterization in the San Juan region, data from seismology, structural geology and quantitative geomorphology were integrated and combined to provide a seismotectonic model. In this seismotectonic model, the Andean back-arc of western Argentina can be regarded as an obliquely converging foreland where Plio-Quaternary deformations are partitioned between strike-slip and thrust motions that are localized on the E-verging, thin-skinned Argentine Precordillera, and the W-verging thick-skinned Sierras Pampeanas, respectively. In this seismotectonic model, the Sierra Pie de Palo appears to be a key structure playing a major role in the partitioning of the Plio-Quaternary deformations.

Keywords: *Seismotectonics, cosmic ray exposure dating, active faulting*

RESUMEN: Tectónica activa en la Precordillera argentina y las Sierras Pampeanas occidentales.

El antepais andino del centro-oeste de Argentina (28°S-33°S) está caracterizado por deformaciones asociadas a la subducción horizontal activa de la placa de Nazca debajo de la litósfera de la placa Sudamericana. En esta región se concentra una importante actividad sísmica y fallamiento cortical activo. Para mejorar la identificación y caracterización de las fuentes sismogénicas en la región de San Juan, fueron integrados y combinados datos de sismología, geología estructural y geomorfología cuantitativa para establecer un modelo sismotectónico. El mismo considera al retroarco del oeste argentino como un antearco con convergencia oblicua donde las deformaciones plio-cuaternarias son particionadas en movimientos compresivos y de transcurrancia dextral.

Dichos movimientos están localizados respectivamente en la Precordillera, una faja de pliegues y escurrimientos de cobertura con vergencia hacia el este, y en las Sierras Pampeanas, una faja de fallas inversas de basamento con vergencia hacia el oeste. Según este modelo sismotectónico, la sierra de Pie de Palo corresponde a una estructura mayor que acomoda la partición de las deformaciones plio-cuaternarias.

Palabras clave: *sismotectónica, edades de exposición por rayos cósmicos, fallas activas.*

INTRODUCTION

The Andean foreland of western Argentina (Fig. 1) of San Juan and Mendoza is among the most seismically active regions in the world. Indeed, many small to moderate ($M < 6.4$) and several large ($M > 6.4$) earthquakes have occurred during the last century, most notably the destructive $M_s = 7.4$, 1944 San Juan earthquake (Instituto Nacional de Prevención Sísmica INPRES 1977, Alvarado and Beck 2006) and $M_w = 7.4$, 1977, Caucete earthquake (Kadinsky-Cade *et al.* 1985; Langer and Bollinger 1988) events. This seismic activity is produced by a number of crustal active faults and may result from the reactivation of ancient sutures between Paleozoic terranes (Smalley *et al.* 1993; Alvarado *et al.* 2005). In the San Juan region, most of the active structures

are related to reverse compressional faulting. Nevertheless, because earthquakes on active reverse faults are not always accompanied with surface ruptures, a paleoseismological estimate of their associated seismic hazard parameters is a difficult task. To improve earthquake source identification and characterization in the San Juan region, data from seismology, structural geology and quantitative geomorphology were integrated and combined to provide a seismotectonic model (Siame *et al.* 2005). In this seismotectonic model, the Present-day tectonic regime is based from inversion (deviatoric stress) and moment tensor sums (strain and seismic rate of deformation) of focal mechanism solutions of moderate to large earthquakes ($M = 5.0$) localized along the Chilean margin and in the Andean foreland. The Neogene-Quaternary tectonic re-

gime rely on inversion of fault plane data (deviatoric stress) and slip rates derived from geological data as well as cosmic ray exposure dating along selected active faults (e.g., Siame *et al.* 1997a,b, 2002). From the comparison of both Present-day and Neogene-Quaternary tectonic regimes, the Andean back-arc of western Argentina can be regarded as an obliquely converging foreland where Plio-Quaternary deformations are partitioned between strike-slip and thrust motions that are localized on the E-verging thin-skinned Argentine Precordillera and the W-verging thick-skinned Sierras Pampeanas, respectively (Siame *et al.* 2005). In this seismotectonic model, the Sierra Pie de Palo appears to be a key structure playing a major role in the Plio-Quaternary deformations within the Andean back-arc at about 31°S.

REGIONAL GEODYNAMIC SETTING

Along the Andes, variations in tectonic style coincide with changes in the geometry of the subducted Nazca plate (e.g., Ramos 1999 and references herein) (Fig. 1). Among those variations, high levels of crustal seismicity characterize the retroarc of the South American plate above flat-slab segments, seismic moment releases being generally 3 or 5 times greater than above 30° dipping segments (Gutscher *et al.* 2000). The Andean foreland of western Argentina (28°S–33°S) corresponds to such back-arc deformation associated with the ongoing subduction of the Pampean flat-slab segment which proceeds nearly horizontally beneath the South American lithosphere

for roughly 300 km at a depth of about 100 km (Cahill and Isacks 1992; Smalley *et al.* 1993). Coinciding with this change of the subducted Nazca plate dip (Jordan *et al.* 1983, Cahill and Isacks 1992), the Andean foreland domain is characterized by two opposite verging, compressional structural provinces coexisting side-by-side: the E-verging, thin-skinned Argentine Precordillera fold-and-thrust belt, and the W-verging, thick-skinned Sierras Pampeanas uplifted basement blocks (Fig. 2). In this Andean region, the flat slab geometry is attributed to the subduction of the Juan Fernandez Ridge below the South American margin (Pilger 1981), and expressed at the magmatic arc by a change in the geochemistry properties of the Neogene volcanism and a cessation of activity roughly 10

Ma ago (Kay and Abbruzzi 1996). Enhanced plate coupling above a flat subduction has long been suggested to be responsible for the large-scale, thick-skinned Sierras Pampeanas basement uplifts (Jordan *et al.* 1983, Smalley *et al.* 1993). On the other hand, thermal weakness of the crust associated with eastward migration of arc magmatism as also been suggested to be responsible for thick-skinned basement uplift of the Sierras Pampeanas (Ramos *et al.* 2002).

Along Chilean margin (Fig. 1) and within the foreland of San Juan (Fig. 2), the Present-day tectonic regime has been investigated thanks to inversions (deviatoric stress) and moment tensor sums (strain and seismic rates of deformation) of focal mechanism solutions (Siame *et al.* 2005). This

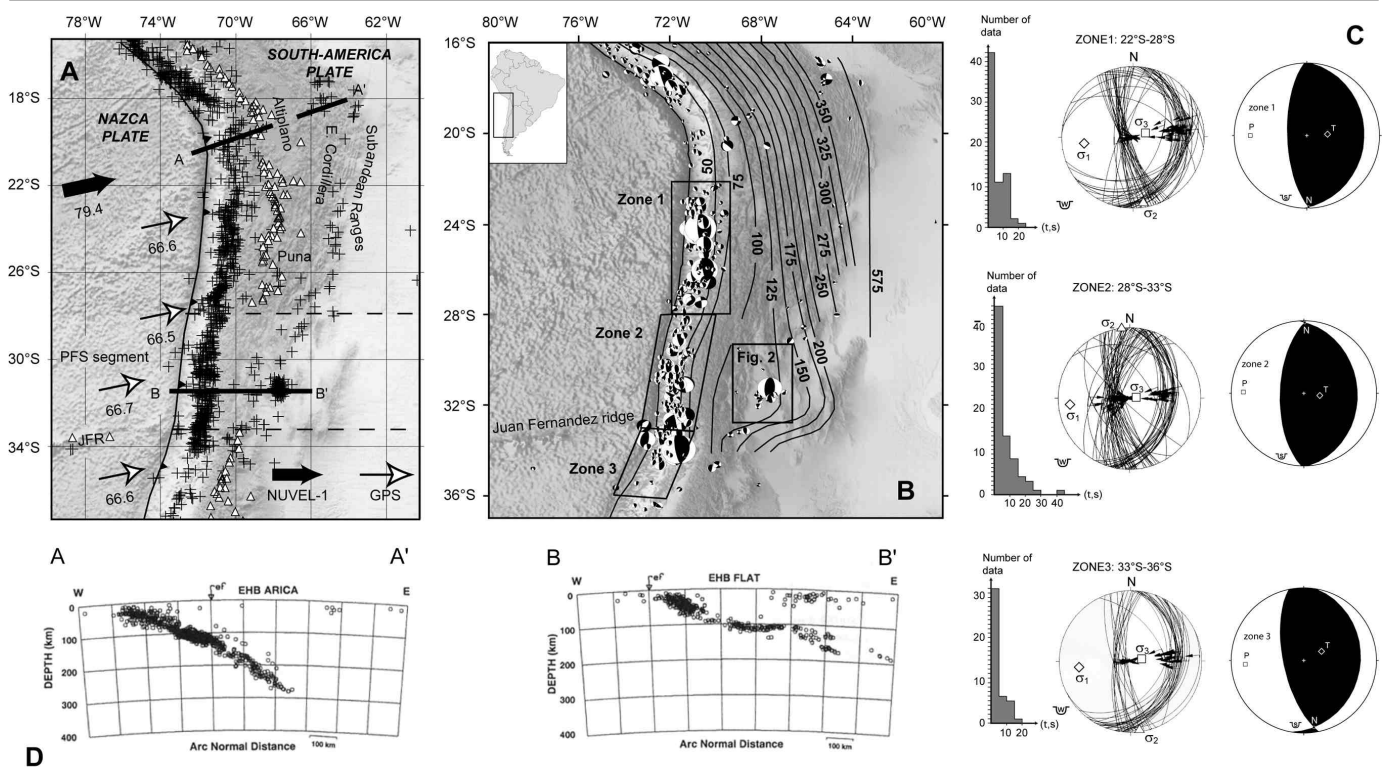


Figure 1: Regional geodynamic setting. a) Map of the central Andes between 19°S and 36°S latitude (Globe shaded relief and bathymetry using Hastings and Dunbar (1998) and Smith and Sandwell (1997), respectively). Black cross represent the epicenter distribution of large to moderate earthquakes (U.S. Geological Survey, National Earthquake Information Center; Preliminary Determination Epicenter catalog, 1973–Present, depth ≤ 70 km, $M \geq 5.0$). Open triangles correspond to Plio-Quaternary and active volcanoes. Black and white arrows represent the relative convergence of the Nazca and South-American plates following NUVEL-1 (DeMets *et al.* 1990, 1994) and continuous GPS observation (Kendrick *et al.* 1999; 2003). Numbers are given in mm/yr. b) Map showing the focal mechanism solutions available in this Andean region from Harvard catalog (1977–2003, depth ≤ 70 km, $M \geq 5.0$). Boxes locate the different zones where inversion and moment tensor sum have been applied along the Chilean trench (e.g., Siame *et al.* 2005). c) Lower-hemisphere stereoplots (Wulf) and synthetic focal solutions (Schmidt) showing inversion and moment tensor sum results, respectively. Histograms show distribution of deviation angles between the selected ' σ ' and the predicted ' τ ' slip-vector on each preferred seismic plane. Stress axes obtained by inversions are shown by diamonds (σ_1), triangles (σ_2) and squares (σ_3). Strain axes obtained by summations are shown by squares (P), and diamonds (T). d) AA' and BB' are cross-sections showing the depth distribution of relocated earthquakes (after Engdahl *et al.* 1998). Keys: PFS, Pampean flat-slab segment; JFR, Juan Fernandez Ridge.

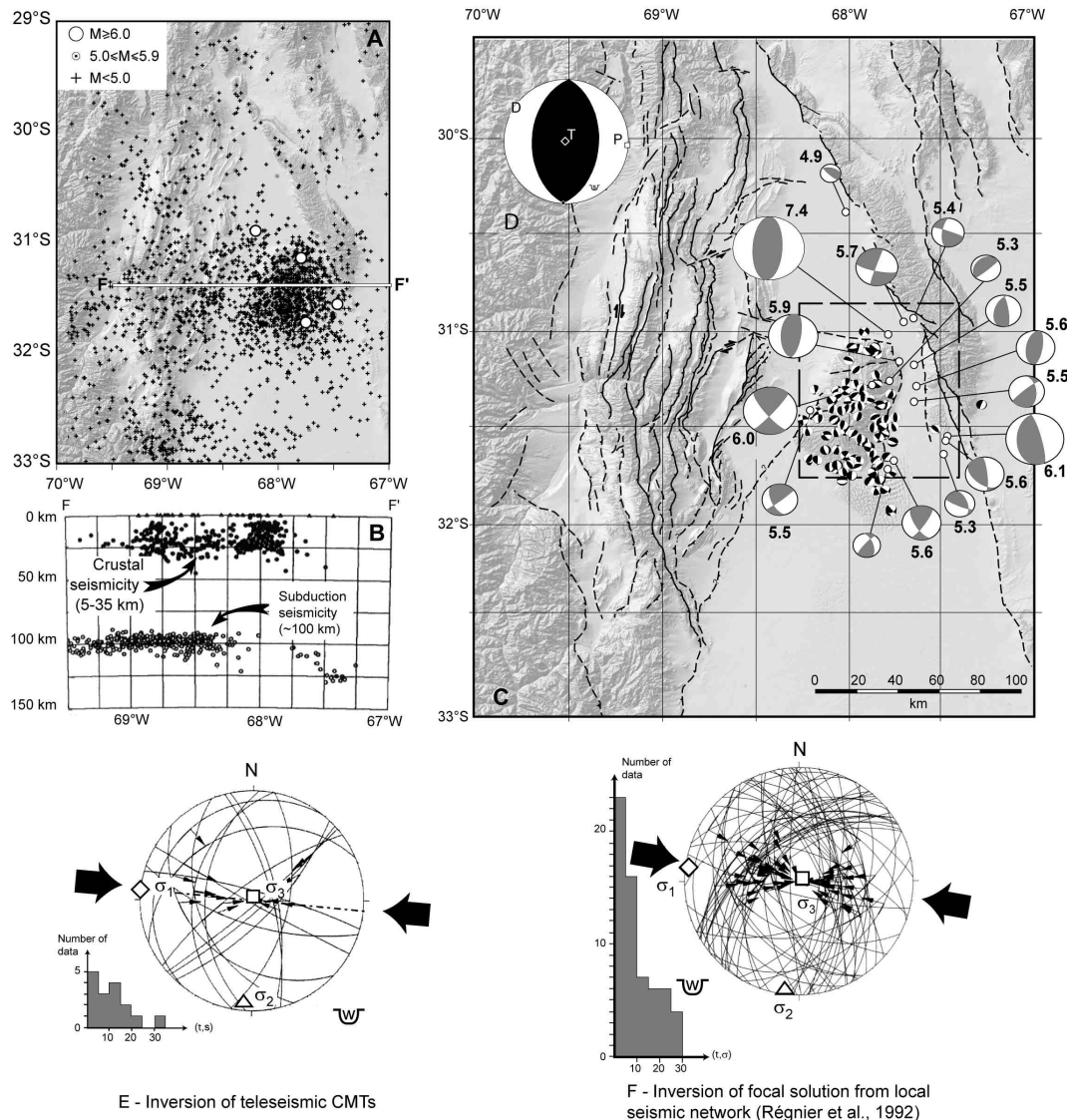


Figure 2: a) Map of San Juan region (shaded relief from SRTM90 digital topography; e.g., Rosen *et al.* 2000; Far and Kobrick, 2000) showing 1973-2003 crustal seismicity from NEIC preliminary determination epicentres and locating cross-section. b) Cross-section (FF') showing shallow (solid circles) and intermediate-depth (open circles) earthquakes (modified after Smalley *et al.* 1993). c) Map of the San Juan foreland domain showing the location of the teleseismic (large grey beachballs; Harvard CMT catalogue) and local (small black beachballs; Régnier *et al.* 1992) focal mechanism solutions used in this study. Black numbers indicate Harvard CMT magnitudes. d) Synthetic focal solution of the moment tensor sum using the Harvard CMT solution (after Siame *et al.* 2005). e) Lower-hemisphere stereoplots (Wulf) showing inversion results for the teleseismic dataset (after Siame *et al.* 2005). f) Lower-hemisphere stereoplots (Wulf) showing inversion results for the local dataset (data after Régnier *et al.* 1992; inversion after Siame *et al.* 2005). Histograms show distribution of deviation angles between the selected 's' and the predicted 'τ' slip-vector on each preferred seismic plane. Stress axes obtained by inversions are shown by diamonds (σ_1), triangles (σ_2) and squares (σ_3).

study raised the following points: (1) the slight convergence obliquity at the plate boundary is accommodated by the subduction zone itself, precluding any deformation partitioning at a lithospheric scale; (2), clockwise rotation of σ_1 -axes and P-axes within the Andean foreland of western Argentina suggest that deformation partitioning may occur in the upper plate at a crustal scale, (3) comparing seismic rates of shallow deformations determined from mo-

derate to large earthquakes localized between 22 and 36°S shows that the amount of shortening is about the same (2-4 cm/yr) between the fore-arcs of the 30° dipping slab segments and the back-arc of the flat segment. Interestingly, the trench segment corresponding to flat subduction is characterized by a much lower seismic moment release during the last 30 years. When compared to the GPS-derived velocity field (elastic strain field) for the Andean Moun-

tains (Kendrick *et al.* 2003, Brook *et al.* 2003), it seems that the clockwise rotation of the stress and strain axes respect to the plate convergence, evidenced from both teleseismic and local focal solutions, may also be seen despite the elastic loading of the upper plate. Whether the strain partitioning suggested by both seismic data and GPS-derived velocity field is recorded at a much longer time scale than the last 30 years has been investigated through the

analysis of the Neogene to Quaternary tectonic regimes (see section 4).

STRUCTURAL OVERVIEW OF THE ANDEAN FORELAND OF SAN JUAN AND MENDOZA (29°S-33°S)

Between 29°S and 33°S latitude, the Andean foreland of San Juan and Mendoza Provinces is characterized by three major N-trending mountainous ranges: The Cordillera Principal, the Cordillera Frontal, the Argentine Precordillera, and the Sierras Pampeanas (Fig. 3). The Cordillera Principal was the first morphostructural unit developed after the Farallones plate break-up and is closely related to the shifting of the Andean orogenic front ever since. The associated mountain building processes ended while the Andean shortening was taking place in the Cordillera Frontal and Precordillera. The Precordillera mountain belt, which is nearly 400 km-long and roughly 80 km-wide, is a thrust-and-fold belt separated from the Cordillera Frontal by an N-S piggyback basin: the Calingasta-Iglesia Valley (Fig. 3). To the east, the Precordillera is flanked by the Bermejo foreland basin that separates the Precordillera thrust-belt from the Sierras Pampeanas, a structural province characterized by ranges uplifted above moderate to highly-dipping, mostly west-verging reverse faults that root deeply into the Precambrian basement rocks (Ramos *et al.* 2002). The structural evolution of this region reflects the regional convergence between the Nazca and South America plates, which led to the formation of the east-verging thin-skinned Precordillera and of the west-verging thick-skinned Sierras Pampeanas, forming two opposite verging structural systems (Figs. 3 and 4) (Jordan *et al.* 1993, Zapata and Allmendinger 1996).

The Cordillera Frontal is the major Andean topographic feature in the studied region, and reaches elevation higher than 5000 m. This mountain belt is mainly composed of a thick Carboniferous to Triassic volcanic rocks and batholiths (Llambias and Caminos 1987), as well as significant Lower and Middle Miocene volcanic rocks (Ramos *et al.* 1986). During the Andean deformation,

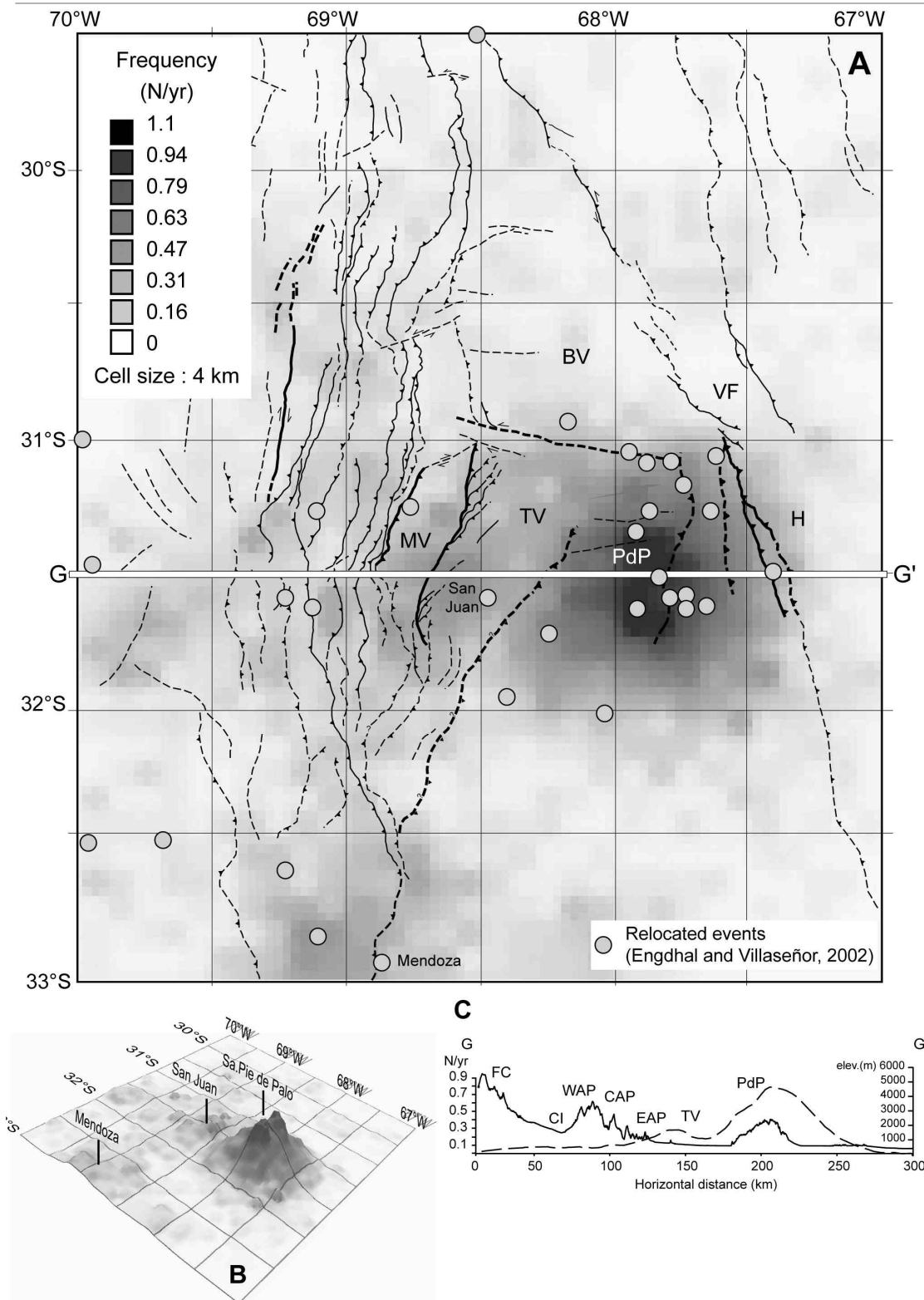
the Cordillera Frontal has apparently behaved as relatively rigid blocks, disrupted by high-angle reverse faults. Allmendinger *et al.* (1990) suggested that, between 29° and 31°S latitude, the Cordillera Frontal is uplifted as a ramp-anticline over a mid-crustal décollement.

The 30 km-wide Calingasta-Iglesia Valley is a piggy-back basin partly filled with Mio-Pliocene sediments and andesites, and Quaternary deposits (Beer *et al.* 1990). The Quaternary sediments are mainly related to Pleistocene to Holocene alluvial fans (Siame *et al.* 1997a). In this basin, the continental strata deposited from ~16 to at least 6 Ma (Beer *et al.* 1990), while crustal shortening was occurring in the Cordillera Frontal and the Precordillera. This basin has been interpreted to have been passively transported above a horizontal décollement that links mid-crustal deformation beneath the Cordillera Frontal with the thin-skinned tectonics in the Precordillera (Beer *et al.* 1990). In the Iglesia valley, the El Tigre Fault is a 120 km-long right-lateral strike-slip fault along which geomorphic features (fan and river offsets, sagponds) and surface disruptions provide evidences for its Quaternary activity (Bastias 1985, Siame *et al.* 1997b, Costa *et al.* 2000 and references herein).

Between 30° and 32°S, the Precordillera is classically divided into three structural provinces: Western, Central, and Eastern (Ortiz and Zambrano 1981, Baldis *et al.* 1982). Western and Central Precordillera correspond to a mountainous topography predominantly characterized by a landscape of linear ranges and basins (Fig. 3). Reverse thrust faults bound Paleozoic ranges and narrow linear valleys filled with Neogene and Quaternary continental sediments (von Gosen 1992, Jordan *et al.* 1993). Western and Central AP have been described as a typical thin-skinned thrust-and-fold belt due to Neogene crustal shortening on west-dipping, imbricated structures that root down to a 10-15 km deep main décollement (Allmendinger *et al.* 1990, von Gosen 1992, Jordan *et al.* 1993, Cristallini and Ramos 1995) (Fig. 2). Formerly, the Eastern Precordillera was grouped in the Precordillera because of its geographic proximity, and mostly because Paleozoic characteristics

(Ortiz and Zambrano 1981, Baldis *et al.* 1982). Nevertheless, since it is thrust westwardly from the craton thanks to faults that reach mid-crustal depths, it can be attributed to the Sierras Pampeanas domain (Zapata and Allmendinger 1996, Jordan *et al.* 2001, Siame *et al.* 2002). The Central and Eastern Precordillera thus form oppositely verging thrust systems on the western and eastern side of the Ullúm-Matagusanos-Huaco valleys (Fig. 3). Conversely to the Western and Central Precordillera, the Eastern Precordillera exhibits a drastic a-long-strike change of structural and geomorphic style at about 31°S latitude (Fig. 3). North of this latitude, the Eastern Precordillera is characterized by thick-skinned, blind thrusts and folds developed within the Neogene strata of the Bermejo valley (Zapata and Allmendinger 1996), whereas it is marked by thick-skinned emergent thrusts carrying mostly Paleozoic rocks to the south (Smalley *et al.* 1993, Siame *et al.* 2002). The location of this change in the structural style of the Eastern Precordillera coincides with the north Pie de Palo Fault (Fig. 3). In fact, it is most probably related to a major change in the basement depth from 8 to 17 km across the southern margin of the Bermejo basin (Jordan and Allmendinger 1986, Smalley *et al.* 1993). South of 31°S latitude, the Eastern Precordillera is bounded by one regional active thrust, the Villicúm-Pedral thrust (Costa *et al.* 2000 and references herein; Siame *et al.* 2002). This thrust system corresponds to a 145 km-long, N20°E-trending fault that runs on the western piedmont of the Eastern Precordillera bounding Sierra de Villicúm, Sierra Chica de Zonda and Sierra de Pedernal (Fig. 3). It is characterized by a surface fault trace that clearly displaces the Quaternary deposit surfaces (Siame *et al.* 2002).

The Bermejo basin is a Miocene to recent foreland basin formed during the development of the Andes and Sierras Pampeanas mountains (Jordan *et al.* 2001). It developed firstly between 20 and approximately 7.3 Ma as a simple foreland basin adjacent to the advancing thrusts of the Western and Central Precordillera (Jordan *et al.* 2001). Then after a short period (<1 Myr) of symmetrical foreland, it developed during the



last 6.5 Ma as an asymmetrical foreland associated with both thin-skinned thrusting in the Central Precordillera and thick-skinned tectonics in the Pampean basement (Jordan *et al.* 2001).

The Sierras Pampeanas are approximately N-trending basement block uplifts of Precambrian metamorphic rocks with topographic characteristics that consist of steep sloped sides on the faulted front and gently

dipping back sides (Fig. 3). The topographic back side corresponds to a Late Palaeozoic erosional basement surface (Carignano *et al.* 1999). The basement blocks are separated by wide, shallow basins of unmeta-

morphosed, relatively undeformed Carboniferous and younger sediments (Salfity and Gorustovitch 1984).

PRESENT-DAY SEISMOTECTONIC REGIME

Within the Andean foreland of western Argentina, earthquake activity is characterized by two depth distributions (Fig. 2). Earthquakes with hypocentral depths at about 100 km show flat slab geometry of the Nazca plate beneath South-America (Cahill and Isacks 1992, Smalley *et al.* 1993, Engdahl *et al.* 1998), whereas earthquakes with hypocentral depth ranging from 5 to 35 km correspond to crustal seismicity between the Argentine Precordillera and the Sierras Pampeanas (Smalley *et al.* 1993). In this region, the crustal seismicity pattern derived from preliminary determination epicentre catalogue (USGS/NEIC) is dominated by a cluster of events centred on the Sierra Pie de Palo (Fig. 2). To efficiently interpret this pattern, we applied a gridding algorithm to the seismic event frequency distribution (Siame *et al.* 2005). The resulting map not only takes into account the dense N-trending ellipsoid-shaped clustering of events centred on the eastern side of the Sierra Pie de Palo, but also clearly unveils two others areas of moderate frequency located near San Juan and Mendoza cities (Fig. 4). Around San Juan city, this zone of moderate frequency corresponds to the Tulum and Matagusanos valleys, where thick-skinned active faulting has been suspected to be responsible for the Ms 7.4, 1944 San Juan earthquake (Smalley *et al.* 1993, Siame *et al.* 2002). The rest of the Precordillera is relatively aseismic, particularly north of the north Sierra Pie de Palo Fault, which is in agreement with epicentre distributions from local seismic networks (Régnier *et al.* 1992, Smalley *et al.* 1993), relocated teleseismic events (Engdahl and Villaseñor 2002), and with the location of the regional active faults (Siame *et al.* 2005). Within the Andean foreland of San Juan, earthquakes with $M_w \geq 4.9$ provide evidence for predominantly reverse to strike-slip faulting (Fig. 2), mostly indicate E-trending shortening on $\sim 40^\circ$ -dipping faults, and have their source depths ranging from 5 to 35

km. From September 1987 to May 1988, Régnier *et al.* (1992) operated a digitally recording seismic network that provided a detailed view of the crustal seismicity in the area (with a maximum activity at about 25 km depth). Even if both seismicity patterns observed from teleseismic and local data are quite similar, teleseismic data are centred on the low-lying valley between Sierra Pie de Palo and Sierra de la Huerta, whereas local data cluster below Sierra Pie de Palo (Fig. 2). This slight difference in the epicentre location is most probably due to systematic differences in location obtained for the two datasets. Best-fitting deviatoric stress tensors from inversions of both teleseismic and local datasets are consistent with σ_1 -axes striking $N95 \pm 2^\circ E$ (Fig. 2). Moment tensor sum of the CMT solutions provide consistent results with P-axes striking $N93^\circ E$ (Fig. 2), parallel to the computed σ_1 -axes. Both inversion and moment tensor sums indicates that σ_1 -axes and P-axes are roughly orthogonal to the strike of the reverse faults that borders the Sierra Pie de Palo basement uplift, and consequently slightly rotated clockwise with respect to the Nazca vs. South American plates convergence trend (Fig. 2). When compared to the GPS-derived velocity field for the Andean Mountains (Kendrick *et al.* 1999, Kendrick *et al.* 2003, Brooks *et al.* 2003), it seems that this clockwise rotation of the stress axes does not only result from local boundary effects within the Sierras Pampeanas, as already suggested by Régnier *et al.* (1992), but may have a more regional significance (Siame *et al.* 2005).

NEOGENE TO QUATERNARY TECTONIC REGIME

STRESS REGIME FROM INVERSIONS OF FAULT SLIP-STRIAE

In order to determine the most recent states of stress within the Precordillera and westernmost Sierras Pampeanas, quantitative inversions of fault slip-vectors (striae) measured at individual in Paleozoic rocks from the Precordillera, in Mesozoic rocks from the Sierras Pampeanas, and in Neogene to Quaternary continental deposits that fill the inter-mountainous and foreland

basins. Some individual sites of measurements are also located on active faults where the computed states of stress can be regarded as significant for recent stress regimes. The results of these quantitative inversions of fault slip-vectors have been presented in details in papers by Siame *et al.* (2002, 2005).

Even if, at individual sites, some of the observed fault-slip data can be related to earlier stress states (e.g., Triassic extension in the Sierras Pampeanas), chronological relationships allowed determining the most recent set of fault slip-vectors to determine the most recent states of stress which are discussed. The stress tensors determined using fault-slip measurements within Paleozoic and Mesozoic rocks from the Precordillera and Sierras Pampeanas are remarkably consistent with the stress tensors deduced from inversion of fault-slip data collected within the Neogene and Quaternary sediments. Compared at a regional scale, the stress regimes determined at individual sites yield a regional stress pattern that is in close agreement with the stress tensors determined using local and teleseismic focal mechanism solutions, as well as with the elastic strain field deduced from the GPS-derived velocity field (e.g., Brooks *et al.* 2003).

In the Precordillera, Paleozoic to Quaternary strata are involved in the deformation, which is related to the Andean (< 20 Myr) structuration of the region. Since the Precordillera developed eastwardly during the last 20 Ma, the fault-slip sites determined for the Western Precordillera are most probably older than those calculated for the Central, Eastern Argentine Precordilleras and Sierras Pampeanas. In the Western and Central Precordillera, where the thrust mainly developed between 20 and 5 Ma (Jordan *et al.* 2001), the stress regime is dominated by σ_1 -axes striking parallel to that determined for the Chilean trench. In the westernmost Sierras Pampeanas and Eastern Precordillera, where the thrust initiated between 5 and 2.5 Myr, the stress regimes are dominated by $N110^\circ E$ -trending σ_1 -axes south of $31^\circ S$, whereas it is striking parallel to that determined for the Chilean trench north of $31^\circ S$ (Fig. 5). When compared to the stress regime pattern to the

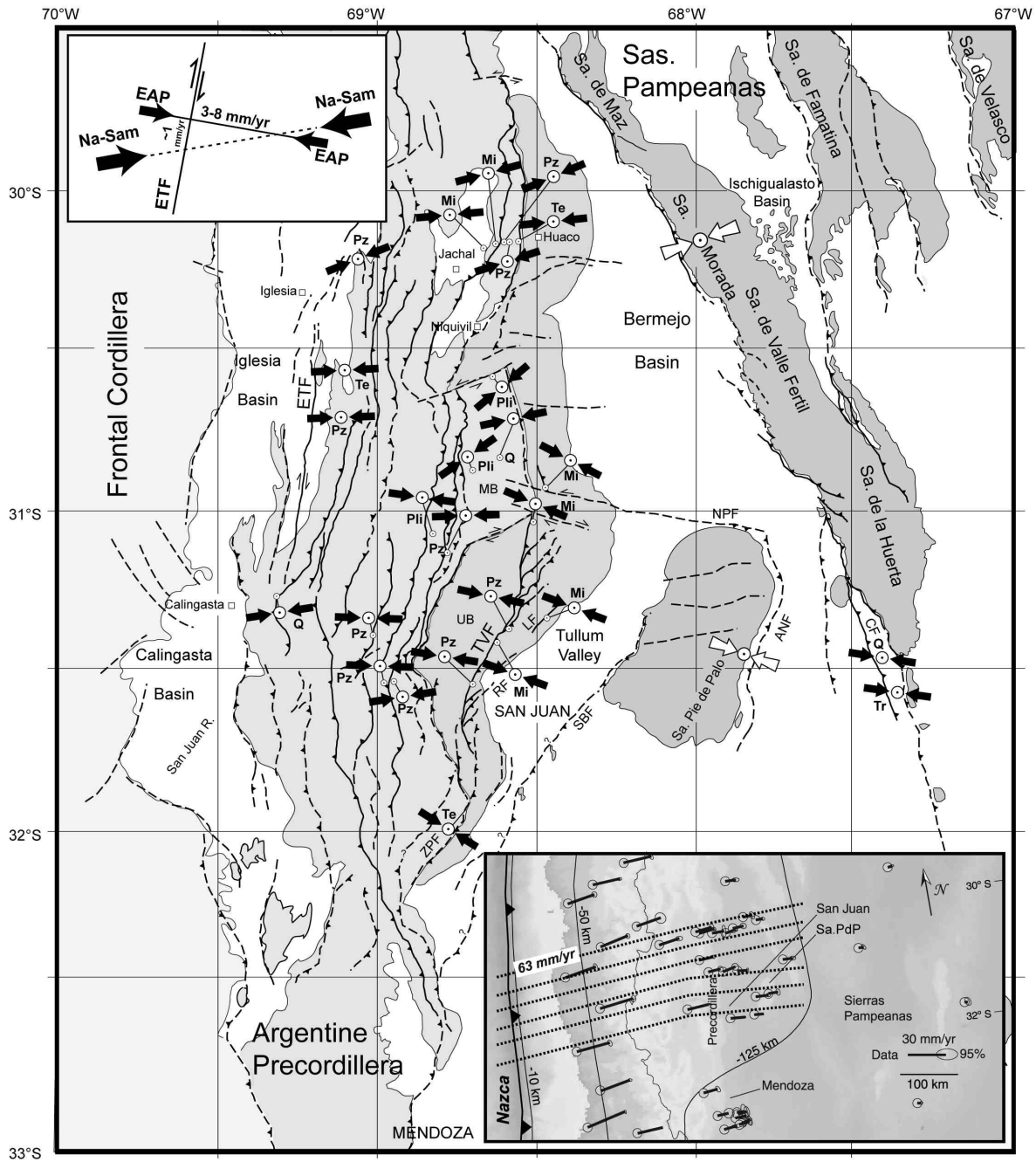


Figure 5: Structural regional map of Argentine Precordillera and western Sierras Pampeanas showing the inversion results of fault kinematic data measured at individual sites (after Siame *et al.* 2005). Black arrows show compressional directions. Keys: Q, Quaternary; Pli, Pliocene; Mi, Miocene; Te, Tertiary; Tr, Trias; Pz, Paleozoic. White arrow (compressional direction) on Pie de Palo shows the inversion result for focal mechanism solutions. White arrow (compressional direction) on Sierra Morada show the compressional direction inferred from regional observations. Upper inset depicts the Plio-Quaternary strain partitioning model for the San Juan foreland domain, lower inset shows the GPS-derived velocity field (modified after Brook *et al.* 2003).

GPS-derived velocity field proposed by Brook *et al.* (2003), the stress regime pattern derived from fault slip-vector data in the Eastern Precordillera and westernmost Sierras Pampeanas are in relative agreement. Indeed, the northern part of the San Juan foreland both σ_1 -axes and GPS-deri-

ved velocity vectors strike in a direction parallel to that of the plate convergence (Fig. 5). Farther south, the comparison is not so conspicuous with GPS-derived velocity vectors striking E-W (Fig. 5). Nevertheless, GPS-derived velocity vectors seem to be also clockwise rotated, suggesting that the

clockwise rotation of σ_1 -axes evidenced from both focal mechanism (Present-day) and fault slip-vector (long-term) datasets may also be seen in the GPS-derived velocity field despite the upper plate elastic loading (Fig. 5).

GEOLOGICAL RATES OF DEFORMATION

Previous study (e.g., Allmendinger *et al.* 1990, Cristallini and Ramos 2000) have shown that Andean orogeny may have resulted in more than 90 km of shortening accommodated by the Precordillera, yielding a mean shortening rate of 5 mm/yr if integrated over the last 20 myrs. Age of shortening in the east-verging AP is relatively well-known at about 30°S (e.g., Jordan *et al.* 1993, Zapata and Allmendinger 1996), whereas it is less constrained at ~31°S. Near 30°S, age and amount of shortening have been estimated mostly through magneto-stratigraphy and growth strata: the Western Precordillera experienced an early phase of shortening roughly 20 Ma ago (rates <5 mm/yr) followed by a period of quiescence (Jordan *et al.* 1993). Thrusting in the Western and Central Precordillera then resumed roughly 15 Ma ago with a period of rapid rates (15-20 mm/yr) spanning at about 10-12 Ma, followed by declining rates (Jordan *et al.* 1993a, Zapata and Allmendinger 1996), even though some of the easternmost thrusts may have been active throughout the Quaternary (Zapata and Allmendinger 1996, Siame 1998). Those previous studies have shown that the deformation front of the AP has experienced a total shortening of ~40 km during the last 5 Myr, implying a mean geological shortening rate of ~8 mm/yr. Regarding the Eastern Precordillera and the Bermejo Valley, they accommodated ~17 km of shortening during the last 3 Myr (Ramos *et al.* 2002), yielding a mean deformation rate of about 6.5 mm/yr. The amount of shortening associated with the Sierra Pie de Palo is on the order of 15 km and may have started between 5 and 3 myrs, yielding a mean shortening rate of 3-5 mm/yr (Ramos *et al.* 2002).

QUATERNARY RATES OF DEFORMATION FROM COSMIC RAY EXPOSURE DATING

In active tectonic studies, quantification of the tectonic forcing processes requires continuous and well-controlled chronologies of the landscape development over long-spanned time scales. Cosmic ray exposure dating

methods have opened new prospects for long term surface processes analysis (e.g., Gosse and Phillips 2001). During the past decade, the cosmic ray exposure dating method provided relatively accurate estimates of the Quaternary deformation rates along active faults in the Andean Foreland of San Juan (Siame *et al.* 1997a, 2002).

HORIZONTAL AND VERTICAL SLIP RATES ASSOCIATED TO THE EL TIGRE FAULT

The El Tigre Fault is a 120 km-long right-lateral strike-slip fault along which geomorphic features (fan and river offsets, sag ponds) and surface disruptions demonstrate its Quaternary activity (Bastias 1985, Siame *et al.* 1997b). The fault is located in the Calingasta-Iglesia Valley which is a 30 km-wide piggyback basin filled with Mio-Pliocene clastic sediments and andesites, and Quaternary deposits (Fig. 3). The El Tigre Fault trace analyzed on SPOT images extends northward from the Río San Juan to the Río Jáchal (Fig. 6), has a mean N10°E-striking, linear and discontinuous fault trace composed by 1 to 7 km-long fault strands. At the surface, this fault zone affects chiefly Tertiary and Quaternary formations as well as some Paleozoic rocks in its southern part. The fault strands are separated by stepovers, bends or relay discontinuities (Fig. 6).

The overall fault geometry may be described considering two to three main segments. The southern segment is 74 km-long, and exhibits a continuous trace, extending from 31.2°S, north of the San Juan River to ~30.9°S (Fig. 6). It is the most pronounced fault segment on SPOT satellite images where it is clearly evidenced by offset stream channels, 200-400 meters wide releasing and restraining stepovers, which are always marked by depressions and pressure ridges, respectively (Fig. 6). From 30.9°S to 30.6°S, the fault trace is also characterized by an east-facing steep slope, commonly bounded by several sag ponds on its eastern foot and by beheaded alluvial fans on its western side (Fig. 6). Southward, the fault trace vanishes within the Precordilleran Paleozoic strata, and may be interpreted as the southern tip of the El Tigre

Fault. On the basis of the fault trace geometry, Siame *et al.* (1997b) proposed to divide the southern segment of the El Tigre Fault into central and southern segments, 26 and 48 km-long, respectively. The northern segment is 46 km-long and extends as far as Rodeo city (30.2°S). Although the N10°E fault strike is preserved, this segment is composed of smaller 1 to 5 km-spaced elementary fault strands, and the surface deformation appears to be more distributed. Considering these numerous spaced fault strands, we interpreted this segment as the northern El Tigre Fault "horse-tail"-like termination (Fig. 6).

Along the southern segment of this active fault, alluvial fans skirting the western piedmont of the Precordillera are incised by a drainage network of stream channels, gullies, and ridges. Most of these geomorphic markers provide evidence for right-lateral displacements, with a maximum offset of 260±20 m cumulated during Late Quaternary. Thanks a geomorphic analysis of the alluvial fan surfaces incised by the deformed drainage network, we estimated that the channel incision took place between the abandonment of the A4 unit and the abandonment of the A3 unit (Fig. 6). Cosmic ray exposure dating of the abandoned fan surfaces allowed constraining an horizontal slip-rate for the ETF of about 1 mm/yr (0.5-2 mm/yr). Along the central segment of the El Tigre Fault, a beheaded series of alluvial fans is uplifted by pressure ridges formed within local fault strands. Cosmic ray exposure dating of these alluvial surfaces yielded a local vertical slip rate on the order of 0.3 mm/yr. The vertical and horizontal slip-rates estimated at roughly 0.3 and 1.0 mm/yr, respectively, yield a reconstructed slip-rake of about 17° for the El Tigre Fault, similar to the fault slip vector observed in a trench on the fault plane (fault plane azimuth: N17°E, dip: 78°E, striae pitch: 14°S).

VERTICAL SLIP RATE ASSOCIATED WITH THE LAS TAPIAS FAULT

The Villicúm-Pedernal thrust is a 145 km-long, N20°E-trending structure that runs on the western piedmont of the Eastern Precordillera between 31°S and 32°20'S lati-

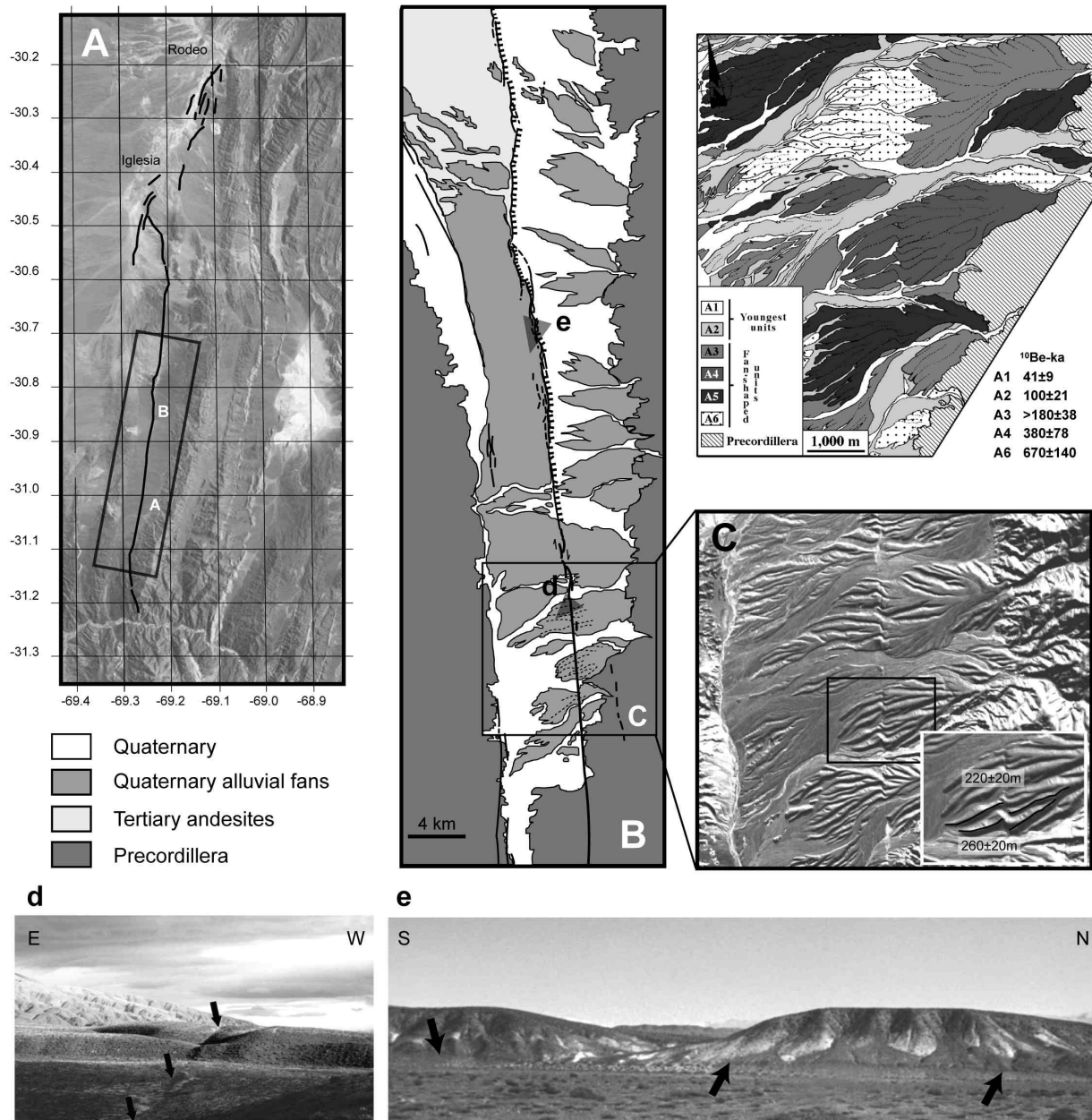


Figure 6 The El Tigre Fault. a) Map of the 120 km-long Quaternary fault trace of the ETF overlain on Landsat TM (after Siame *et al.* 1997b). b) This figure presents partly the ETF southern and central segments (after Siame *et al.* 1997b), locates inset c and field photographs (d, e). c) The southern segment. It is composed of a unique trace which cross-cuts Quaternary alluvial fans where displaced geomorphic features can be observed. The color map presents the Quaternary alluvial fan deposits from field observations and panchromatic (10 m/pixel) SPOT image interpretation. The numbers refer to the minimum surface exposure ages calculated from ^{10}Be concentrations measured in surface boulders (Siame *et al.* 1997a). Spot image extract shows the maximum horizontal cumulative displacements recorded by the drainage network. d) field photograph presenting the ETF trace (black arrows) in the landscape along the central segment. e) Field photograph presenting the ETF trace (black arrows) in the landscape along the southern segment

tude (Fig. 3), bounding Sierra de Villicúm, Sierra Chica de Zonda and Sierra de Pederal (Fig. 7). Structural segments separated by oblique N40°E-trending fault branches define the Villicúm-Pederal thrust. These segments are the Villicúm, the Las Tapias, and the Zonda-Pederal segments, from north to south, respectively. Both the Villi-

cúm and Las Tapias segments are characterized by a fault trace that clearly affects the Quaternary deposits whereas, the fault trace of Zonda-Pederal segment is less conspicuous (Siame *et al.* 2002).

The Las Tapias Fault is 18 km-long and extends with the same N22°E trend between the southern Sierra de Villicúm and the

northern Sierra Chica de Zonda fault branches. In the low-lying region localized between the Sierra de Villicúm and the Sierra Chica de Zonda, the Las Tapias Fault affects Quaternary alluvial deposits that overly unconformably the Neogene foreland strata and forms discontinuous and degraded west-facing scarps (Fig. 7). Minor

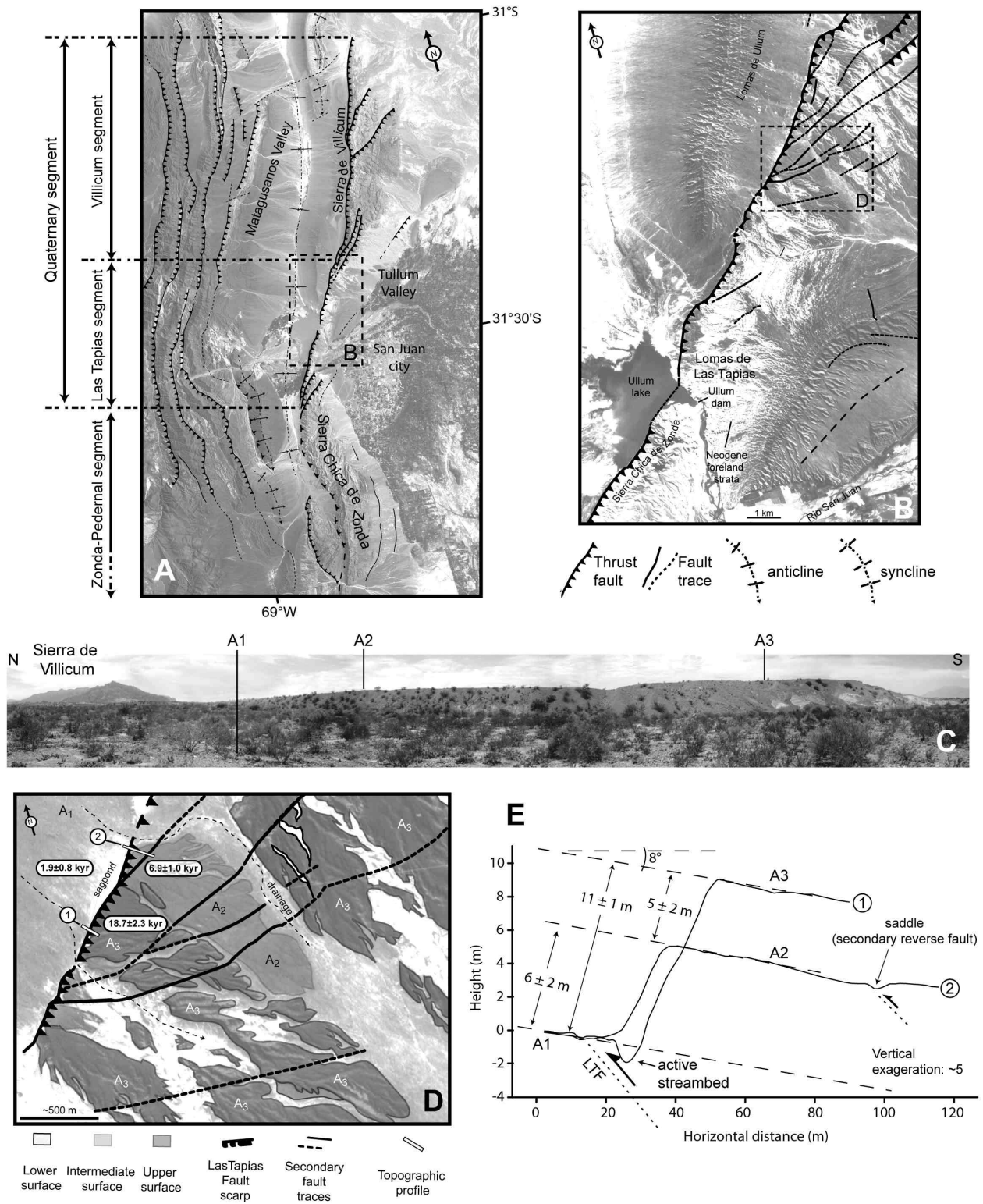


Figure 7: The Las Tapias Fault. a) Structural map of the 65 km-long Quaternary segment of the Villicum-Pedral thrust overlain on Landsat TM (after Siame *et al.* 2002). b) Structural map of the Las Tapias Fault shown on an aerial photograph centered on the low-lying region between Sierra de Villicum and Sierra Chica de Zonda (after Siame *et al.* 2002). c) Panoramic view of the Las Tapias Fault escarpment showing the three different alluvial levels. d) Map of the alluvial deposits affected by the Las Tapias Fault based on both stratigraphic relationships and surficial morphology observed in the field and on aerial photograph. The numbers refer to the minimum surface exposure ages calculated from ^{10}Be concentrations measured in surface boulders (Siame *et al.* 2002). e) N110°E-striking topographic profiles constructed perpendicularly to the Las Tapias scarps (circled numbers refer to locations on d).

N40°E-trending topographic features, marked by roughly 1 m-high, and 1 to 5 km-long scarps, also affect the Quaternary deposits in the Las Tapias Fault area. These topographic features strike obliquely to the major N22°E-trending Las Tapias Fault and can be regarded as the continuation, within the Quaternary deposits, of the N40°E-trending oblique faults that affect the southern end of Sierra de Villicúm. Both sets of faults at the southern Sierra de Villicúm and the northern Sierra Chica de Zonda are bedding-parallel, and interpreted as flexural-slip faults.

Along strike, the Las Tapias Fault forms west facing, ~10 m-high discontinuous and degraded scarps which affect Quaternary alluvial sediments (Fig. 7). The scarps are west facing, which leads to pounding on the footwall of clastic deposits transported from Loma de Ullúm. Streambeds are draining across the scarps from east to west such that the thrust scarps grown against main drainage. Nevertheless, the interaction of alluvial cutting and recurrent surface faulting has generated a strath terrace sequence that records the faulting history on the hanging wall. Stream gradients are relatively high (<8°), and recurrent faulting on the Las Tapias Fault sufficiently raised the hanging wall to produce a significant vertical down cutting. This stream incision into the up-thrown block has isolated a couple of alluvial terraces that end abruptly at the fault scarp. These terraces can be easily distinguished by their differential elevations, as well as by the difference of both incision pattern and incision degree at their surfaces (Fig. 7). The clastic source for alluvial material is the relief of Loma de Ullúm, and the streams flow direction is roughly SW-NE (Fig. 7). The piedmont is still active as suggested by both a well-developed network of braided streambeds incised ~0.5 m into it, and a well-preserved surface morphology with bars and swales formed by slightly varnished abraded boulders and sub angular cobbles. In an attempt to establish absolute ages for this stratigraphically-based chronology, terrace surfaces have been sampled for cosmic ray exposure dating. Based on the cosmic ray exposure ages published by Siame *et al.* (2002), we propose a minimum CRE age of 1.9 ± 0.8 ¹⁰Be-kyr for the pied-

mont surface, and best proxies for the actual abandonment ages of 6.9 ± 1.0 and 18.7 ± 2.3 ¹⁰Be-kyr for the uplifted surfaces, respectively (Fig. 7).

The displaced alluvial deposits geometry with respect to the fault scarps has been studied to estimate the uplift rate for the hanging wall of the Las Tapias Fault. Indeed, the uplifted terraces result from episodic fault incision into the up-thrown block of the Las Tapias Fault. The vertical separation between the projections of these terraces, measured at the inferred fault plane may thus provide a first approximation of the vertical component of fault displacement. To constrain the vertical component of fault displacement, three topographic profiles have been surveyed perpendicular to the fault trace (Fig. 7). The scarps bounding A2 and A3 terraces have been constructed through time by repeated faulting on the Las Tapias Fault. Since topographic profiles provide constraints on minimum vertical displacement between the geomorphic surfaces and ¹⁰Be cosmic ray exposure ages provide lower limits for time elapsed since surface abandonment, these data allow estimating lower limits for the long-term uplift rate. All together, these estimates yield to a mean uplift and shortening rate of 0.7 ± 0.3 mm/yr and 0.8 ± 0.5 mm/yr, respectively (Siame *et al.* 2002, 2005). This shortening rate is consistent with the ~1 mm/yr shortening rate determined further north over the past 3 Myr by Zapata and Allmendinger (1996) across Eastern Precordillera and Bermejo basin individual structures.

THE ROLE OF THE SIERRA PIE DE PALO

Within the structural context of the Andean back-arc at about 31°S, the Sierra Pie de Palo appears to play a key role in the partitioning of the Plio-Quaternary deformations. Located in the westernmost Sierras Pampeanas, the Sierra Pie de Palo is roughly NNE-striking. It forms an 80 km-long and 35-40 km-wide, ellipsoid shape that reaches elevation as high as 3162 m (Fig. 3 and Fig. 5). This mountain range is an actively growing basement fold (e.g., Ramos *et al.* 2002) associated with an

important seismotectonic activity (Fig. 4). In this area, evidences of Quaternary active deformation are found along the eastern and northern borders of the Sierra Pie de Palo as well as along the western borders of the Sierra de Valle Fértil and Sierra de la Huerta (Fig. 8) (Costa *et al.* 2000, Siame *et al.* 2002, Siame *et al.* 2005). With a dissymmetrical arch-like shape (Fig. 4), its topography is characterized by steep-sloped sides on the eastern and northern fronts and western and southern gently dipping back sides (Fig. 4). The surface envelope of Sierra Pie de Palo corresponds to an inherited, Late Paleozoic erosional surface (Carignano *et al.* 1999) affecting in Precambrian metamorphic rocks. Since, geologic evidence indicates that the range was covered by Late Pliocene distal synorogenic deposits derived from the Precordillera (Ramos and Vujovich 2000), the deformation associated with the growth of the Sierra Pie de Palo may have started between 5 and 3 Myr (Ramos *et al.* 2002). The eastern and western flanks of the Sierra Pie de Palo are characterized by east-dipping and west-dipping Pliocene strata, respectively, indicating that the surface structure of Pie de Palo is characterized by a basement fold (Ramos *et al.* 2002). This basement structure passively folded the Pliocene strata and the unconformity that separates them from the basement, in a similar way than other Sierras Pampeanas (García and George 2004). Based on that, Ramos *et al.* (2002) proposed that the structure is controlled by a basement wedge detached at about 15-20 km depth (Fig. 3), according to the crustal seismicity provided by a local network (Régnier *et al.* 1992). In this context, the role of the Niquizanga Fault (ANF) is still unclear. Indeed, at depth this fault may correspond to a west-dipping, thick-skinned reverse structure that most probably ruptured during the 1977 Caucete earthquake (Kadinsky-Cade *et al.* 1985, Langer and Bollinger 1988). However, it produced very little surface ruptures, suggesting that this fault is mostly buried. Indeed, along the eastern flank of Sierra Pie de Palo, the Pliocene beds are dipping to the east, and near Niquizanga, those strata are slightly folded and unaffected by the fault (V. Ramos, personal comm.). To explain these observa-

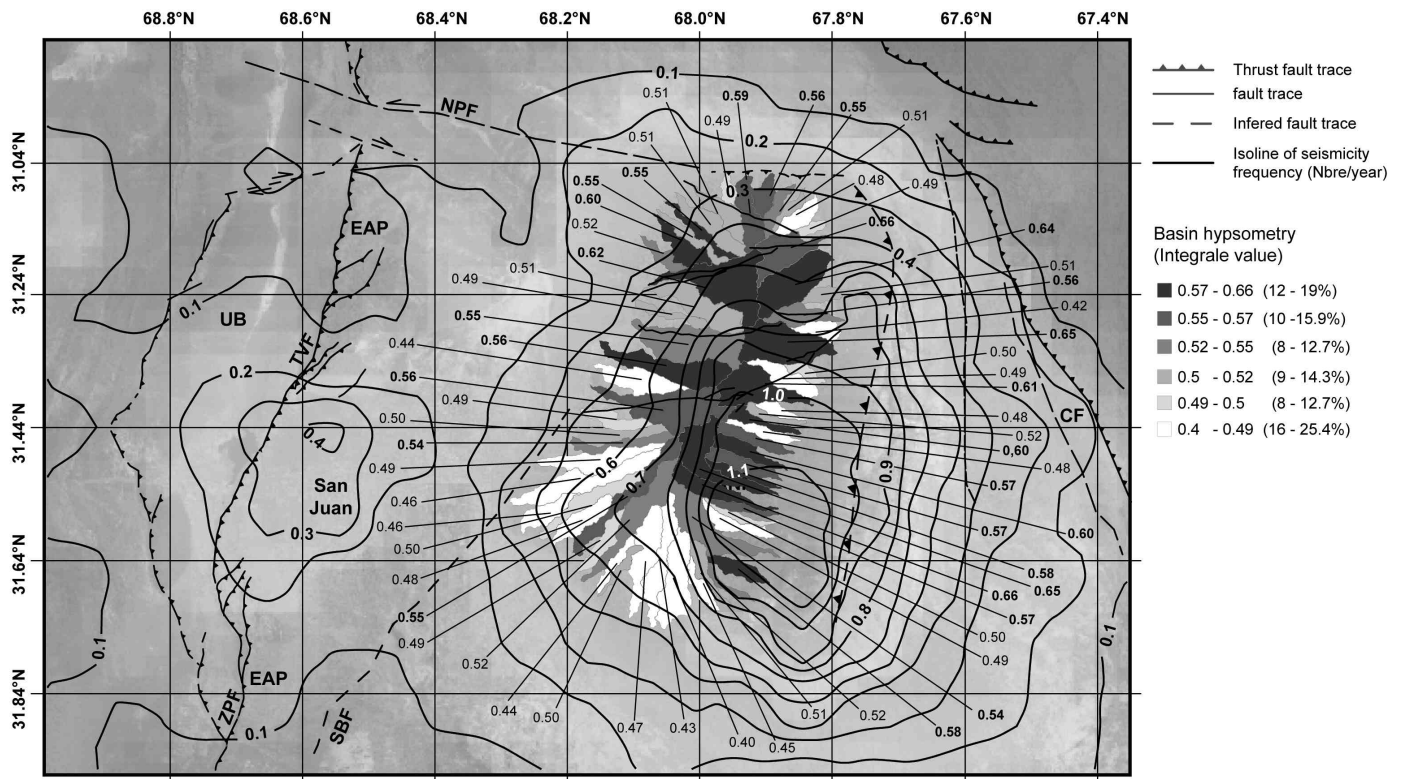


Figure 8: Active tectonics associated with the Sierra Pie de Palo. This map presents the surface fault traces associated to the active structures of the Eastern Precordillera and westernmost Sierras Pampeanas (after Siame 1998, Costa *et al.* 2000, Siame *et al.* 2002, 2005). Shaded area and black solid isolines present the gridded regional seismicity frequency (e.g., Fig. 4). The drainage basins that contribute to the dissection of the surface envelope of the Sierra Pie de Palo are mapped with grey levels according to their hypsometric integral values.

tions, Ramos *et al.* (2002) have proposed that east-dipping faults along the eastern border of Sierra Pie de Palo might be related to W-verging, thick-skinned fault propagation associated to the Sierra de la Huerta and Sierra Valle Fértil. However, such a W-verging thick-skinned propagation would necessarily have produced a significant relief instead of the subsiding Bermejo valley. To our opinion, even if buried along most of its length, an E-verging, Niquizanga Fault system should be regarded as the structure responsible for the dissymmetrical, long-wave length shape of the surface envelope of the Sierra Pie de Palo (Fig. 3).

To evaluate the degree of tectonic activity around the Sierra Pie de Palo, some geomorphic lines of evidence can be drawn from the study of the drainage network. Indeed, even if the lithological and climatic conditions (semi-arid climate) contributed to a good preservation of its surface envelope, the Sierra Pie de Palo is dissected by fluvial incision. Moreover, taking into account that the lithological conditions are

fairly constant throughout the whole area, any active tectonic perturbation should thus be discriminated using the geomorphic indices associated to the drainage network that dissects the Sierra Pie de Palo. Among those geomorphic indices, the hypsometric integral value, related to the degree of dissection of a given landscape, is commonly used to discriminate between tectonically active and inactive regions (Strahler 1952). Indeed, high values of the hypsometric integral (i.e., values close to 1) indicate youthful topographies whereas intermediate to low values (i.e., values close to 0) are related to more matured and dissected landscapes. In the Sierra Pie de Palo, one can consider that the hypsometric integral value of a given drainage basin is directly related to its degree of tectonic activity. The figure 8 presents a map of the drainage basins together with the hypsometric integral values calculated using the SRTM90 digital topography (e.g., Rosen *et al.* 2000, Far and Kobrick, 2000). This morphometric approach unveils that the drainage basins with high va-

lues of hypsometric integral are preferentially located along the northern and eastern borders of the Sierra Pie de Palo. Moreover, along the eastern border, the drainage basins show rectilinear shapes that correlate the seismicity frequency (see above), and the steep slope that characterizes this side of the Sierra Pie de Palo. Considering these combined observations, and the November 23, 1977, Caucete, earthquake sequence (Kadinsky-Cade *et al.* 1985, Langer and Bollinger 1988), it appears that the eastern and northern flanks of the Sierra Pie de Palo are probably among the most active zones in the area.

DISCUSSION OF A SEISMOTECTONIC MODEL FOR THE ANDEAN FORELAND OF SAN JUAN AND MENDOZA

The Andean back-arc of western Argentina can be regarded as an obliquely converging foreland where Plio-Quaternary deformations are partitioned between strike-slip and

thrust motions that are localized on the E-verging thin-skinned Argentine Precordillera and the W-verging thick-skinned Sierras Pampeanas, respectively. In this partitioning model the El Tigre Fault, Eastern Precordillera and western Sierras Pampeanas faults play important roles. The El Tigre Fault geometry and segmentation is tightly associated with the geometry of the Precordillera ranges. Indeed, slight variations of strike in the Precordillera range appear to parallel the El Tigre Fault geometry and discontinuities (Siame *et al.* 1997b). For example, the southern termination of the El Tigre Fault coincides with the Precordillera ranges bending from N160°E to N10°E close to Río San Juan. Along its northern segment, the El Tigre Fault steps westwardly, splaying as a horse-tail termination, coinciding to another orientation change of the Precordilleran ranges (Fig. 5). Among others, these observations lead Siame *et al.* (1997b) to propose that the El Tigre Fault may correspond to a crustal-scale strike-slip fault, closely related to the Precordilleran fold-and-thrust belt. In this Plio-Quaternary transpressive system, the El Tigre Fault should accommodate the dextral strike-slip component while the Eastern Precordillera-Pampean thrusts should accommodate N110°E-trending shortening (Fig. 5). Indeed, if one assumes that the convergence obliquity is regionally accommodated by the El Tigre Fault, Quaternary slip-rates estimated thanks to cosmic ray exposure dating (~1 mm/yr) imply that 3–8 mm/yr of shortening have to be accommodated throughout the Eastern Precordillera-Pampean system in a N110°E-trending direction (Fig. 5). Interestingly, this direction corresponds to the orientation of the σ_1 -axes computed from both focal mechanism (Present-day) and fault kinematic (long-term) datasets within the Eastern Precordillera and westernmost Sierras Pampeanas. This direction also coincides with the trend of the North Pie de Palo Fault that marks the northern limit of the growing Sierra Pie de Palo (Fig. 3), and corresponds to a regional structure playing a major role regarding the seismicity distribution pattern (Fig. 2 and Fig. 4). In our partitioning model, the estimated range of Quaternary shortening rates (3–8

mm/yr) is in close agreement with the geological rates estimated from crustal balancing studies (e.g., Allmendinger *et al.* 1990, Cristallini and Ramos 2000). Since this range of shortening rates has to be distributed over several active thrusts, it is also consistent with a minimum shortening rate of 0.8 ± 0.5 mm/yr determined for the Las Tapias Fault of the Eastern Precordillera south of 31°S over the Holocene period (Siame *et al.* 2002). Even if one argued as to the degree to which the GPS data are accurate, these data suggest that, south of 31°S, 7–9 mm/yr of E-trending shortening have to be accommodated between the Calingasta Valley and Sierra Pie de Palo, with about 4 mm/yr between Eastern Precordillera and Sierra Pie de Palo (Brook *et al.* 2003). Those GPS-derived shortening estimates are thus slightly higher than the long-term geological and Quaternary rates. Moreover, north of 31°S, GPS data suggest that only 2–3 mm/yr are accommodated between the western Precordillera and the Sierra de Valle Fértil, with less than 1 mm/yr within the Bermejo valley. GPS-data thus seem to confirm that most of the Present-day tectonic activity is concentrated south of 31°S, in the Sierra Pie de Palo area. In this context, the shortening rate estimated from seismic moment tensor sum appears to be one order of magnitude greater (3–4 cm/yr) than those estimated above from the GPS-derived velocity field (Siame *et al.* 2002, 2005). This high rate of co-seismic shortening strongly suggests that the November 23, 1977, Caucete, earthquake sequence may have released the elastic deformation accumulated in this region, the high discrepancy with GPS-derived and geological shortening rates being much probably due to the too short-spanned time window. South of 31°S, the regional compressional stress regime is dominated by N110 ± 10°E-trending σ_1 -axis perpendicular to the trend of the Sierra Pie de Palo, and parallel to the trend of the north Pie de Palo Fault (Fig. 5). In this context, the process of basement uplift that exhumed the Sierra Pie de Palo has most probably triggered the regional clockwise reorientation of the compressional axes, observed at the long-term (fault striae) and short-term (seismicity) time windows. This may have started 5–3 Myr ago, that is

to say since the Sierra Pie de Palo is actively growing.

ACKNOWLEDGEMENT

We thank M. Araujo at the INPRES for fieldwork facilities and fruitful discussions, M. Perez and G. Racciopi for helpful assistance during fieldwork. We thank IFEA for travel grants. SPOT images were provided by the Tectoscope-Andes and ISIS programs (CNES/INSU/CNRS) Funding for the CRE analyses was partly provided by the PROSE programme (CNRS-INSU). The CNRS, CEA and IN2P3 support the Tandétron (French ASM facility, Gif-sur-Yvette, France) operation. The authors also thank V. Ramos for fruitful discussions and constructive comments about Sierra Pie de Palo, and J. Cortés and D. Ragona for reviewing their manuscript.

WORKS CITED IN THE TEXT

- Allmendinger, R. W., Figueroa, D., Snyder, D., Beer, J., Mpodozis, C. and Isacks, B. L. 1990. Foreland shortening and crustal balancing in the Andes at 30°S Latitude. *Tectonics* 9: 789–809.
- Alvarado, P. and Beck, S. 2006. Source characterization of the San Juan (Argentina) crustal earthquake of 15 January 1944 (Mw 7.0) and 11 June 1952 (Mw 6.8). *Earth and Planetary Science Letters* (doi: 10.1016/j.epsl.2006.01.015).
- Alvarado, P., Beck, S., Zandt G., Araujo, M. and Triep, E. 2005. Crustal deformation in the south-central Andes back-arc terranes as viewed from regional broad-band seismic waveform modelling. *Geophysical Journal International* (doi: 10.1111/j.1365-246X.2005.02759.x): 1–19.
- Baldis, B.A., Beresi, M.S., Bordonaro, O. and Vaca A. 1982. Síntesis evolutiva de la Precordillera de Argentina. 5° Congreso Latinoamericano de Geología (Buenos Aires), Actas: 31–42.
- Bastias, H. 1985. Fallamiento Cuaternario en la región sismotectónica de precordillera: San Juan, Argentina. Tesis Doctoral, Facultad de Ciencias Exactas, Físicas y Naturales, Universidad Nacional de San Juan, inédita, 160 p.
- Beer, J.A., Allmendinger, R.W., Figueroa, D.A. and Jordan T.E. 1990. Seismic stratigraphy of

- a Neogene piggy-back basin, Argentina. *American Association of Petroleum Geology Bulletin* 74: 1183-1202.
- Brooks, B.J., Bevis, M., Smalley, R., Kendrick, E., Manceda, R., Lauría, E., Maturana, R. and Araujo, M. 2003. Crustal motion in the Southern Andes (26°-36°S): Do the Andes behave like a microplate? *Geochemistry, Geophysics, Geosystems* 4 (10): 14 p.
- Cahill, T., Isacks, B. 1992. Seismicity and shape of the subducted Nazca plate. *Journal of Geophysical Research* 97: 17503-17529.
- Carignano C. Cioccale, M. and Rabassa, J. 1999. Landscape antiquity of the Central Eastern Sierras Pampeanas (Argentina): Geomorphological evolution since Gondwanic times. *Zeitschrift für Geomorphologie* 118: 245-268.
- Costa, C., Machette, M.N., Dart, R.L., Bastias, H.E., Paredes, J.D., Perucca, L.P., Tello, G.E., Haller, K.M. 2000. Map and database of Quaternary faults and folds in Argentina. U.S. Geological Survey Open-file report 00-0108, 81 p., one map.
- Cristallini, E.O. and Ramos, V.A. 2000. Thick-skinned and thin-skinned thrusting in La Ramada fold and thrust belt: Crustal evolution of the High Andes of San Juan, Argentina (32° SL). *Tectonophysics* 317: 205-235.
- DeMets, C., Gordon, D.F. Argus, D.F. and Stein, S. 1994. Effect of recent revisions of the geomagnetic reversal time scale on estimates of current plate motions. *Geophysical Research Letters* 21: 2191-2194.
- DeMets, C., Gordon, R.G. Argus, D.F. Stein, S., 1990. Current plate motions. *Geophysical Journal International* 101: 425-478.
- Engdahl, E.R., van der Hilst, R. and Buland, R. 1998. Global teleseismic earthquake relocation with improved travel times and procedures for depth determination. *Bulletin of the Seismological Society of America* 88: 722-743.
- Engdahl, E. R. and Villaseñor, A. 2002. Global seismicity: 1900-1999. In W.H.K. Lee, H. Kanamori, P.C. Jennings, and C. Kisslinger (editors). *International handbook of earthquake engineering and seismology*, International Geophysics Series 81A: (665- 690).
- Farr, T.G. and Kobrick, M. 2000. Shuttle Radar Topography Mission produces a wealth of data. *American Geophysical Union EOS* 81: 583-585.
- García, P.E. and George H. D. 2004. Evidence and mechanisms for folding of granite, Sierra de Hualfin basement-cored uplift, northwest Argentina. *American Association of Petroleum Geology Bulletin* 88: 1255-1276.
- Gosen (von), W. 1992. Structural evolution of the Argentine Precordillera: The Río San Juan section. *Journal of Structural Geology* 14: 643-667.
- Gosse, J.C., and Phillips, F.M. 2001. Terrestrial in situ cosmogenic nuclides: theory and applications. *Quaternary Science Reviews* 20(14): 1475-1560.
- Gutscher, M.A., Spakman, W., Bijwaard, H. and Engdahl, E.R. 2000. Geodynamics of flat subduction: Seismicity and tomographic constraints from the Andean margin. *Tectonics* 19(5): 814-833.
- Hastings, D.A. and Dunbar, P.K. 1998. Development and assessment of the Global Land One-km base digital elevation model (GLOBE). *ISPRS archives* 32, 4, 218-221.
- Jackson, J., McKenzie, D. 1988. The relationship between plate motions and seismic moment tensors, and the rates of active deformation in the Mediterranean and Middle East. *Geophysical Journal* 93: 45-73.
- Instituto Nacional de Prevención Sísmica (INPRES) 1977. *Zonificación Sísmica de la República Argentina*, Publicación Técnica 5, San Juan.
- Instituto Nacional de Prevención Sísmica (INPRES) 1982. *Microzonificación Sísmica del Valle de Tulum - Provincia de San Juan*, Informe Técnico General, 120 p., San Juan.
- Jordan, T. E. and Allmendinger, R. W. 1986. The Sierras Pampeanas of Argentina: A modern analogue of Rocky Mountain foreland deformation. *American Journal of Science* 286: 737-764.
- Jordan, T.E., Schlunegger, F. and Cardozo, N. 2001. Unsteady and spatially variable evolution of the Neogene Andean Bermejo foreland basin, Argentina. *Journal South American Earth Sciences* 14: 775-798.
- Jordan, T.E., Allmendinger, R.W., Damanti, J.F. and Drake, R. 1993. Chronology of motion in a complete thrust belt: the Precordillera, 30-31°S, Andes Mountains. *Journal of Geology* 101: 135-156.
- Jordan, T.E., Isacks, B., Ramos, V.A. and Allmendinger, R.W. 1983. Mountain building in the Central Andes. *Episodes* 3: 20-26.
- Kadinsky-Cade, M., Reilinger, R., Isacks, B.L. 1985. Surface deformation associated with the November 23, 1977, Cauçete, Argentina earthquake sequence. *Journal of Geophysical Research* 90: 12691-12700.
- Kay, S.M. and Abbruzzi, J.M. 1996. Magmatic evidence for Neogene lithospheric evolution of the Central Andean "flat-slab" between 30° and 32°S. *Tectonophysics* 259: 15-28.
- Kendrick, E., Bevis, M., Smalley, R., Brooks, B.J., Barriga Vargas, R., Lauría, E., Souto Fortes, L.P. 2003. The Nazca-South America Euler vector and its rate of change. *Journal of South American Earth Sciences* 16: 125-131.
- Kendrick, E., Bevis, M., Smalley, R., Cifuentes, O., Galban, F. 1999. Current rates of convergence across the Central Andes: estimates from continuous GPS observations. *Geophysical Research Letters* 26(5): 541-544.
- Langer, C.J. and Bollinger, G.A. 1988. Aftershocks of the western Argentina (Cauçete) earthquake of 23 November 1977: some tectonic implications. *Tectonophysics* 148: 131-146.
- Llambias, E.J. and Caminos, R. 1987. El magmatismo neopaleozoico de Argentina. In S. Archangelsky (ed.) *The Carboniferous system of Argentina*. Publicación especial, Academia Nacional de Ciencias: 253-271, Córdoba.
- Ortiz, A. and Zambrano, J.J. 1981. La provincia geológica Precordillera Oriental. 8° Congreso Geológico Argentino (San Luis), Actas 3: 59-74.
- Pilger, R.H. 1981. Plate reconstructions, aseismic ridges, and low angle subduction beneath the Andes. *Geological Society of America Bulletin* 92: 448-456.
- Ramos, V.A. 1999. Plate tectonic setting of the Andean Cordillera. *Episodes* 22 (3): 183-190.
- Ramos, V. and G. Vujovich 2000. Hoja Geológica San Juan, escala 1:250.000. Servicio Geológico Minero Argentino, Boletín 245, 82 p., Buenos Aires.
- Ramos, V.A., Cristallini, E.O. and Pérez, D.J. 2002. The Pampean flat-slab of the Central Andes. *Journal of South American Earth Sciences* 15: 59-78.
- Ramos, V. A., Jordan, T. E., Allmendinger, R. W., Mpodozis, C., Kay, S. M., Cortés, J. M. and Palma, M. 1986. Paleozoic terranes of the central Argentine-Chilean Andes. *Tectonics* 5: 855-880.
- Régner, M., Chatelain, J.-L., Smalley R., Chiu, J.-M., Isacks, B.L. and Araujo, M. 1992. Seismotectonics of Sierra Pie de Palo, a basement block uplift in the Andean Foreland of

- Argentina. *Bulletin of the Seismological Society of America* 82 (6): 2549-2571.
- Rosen, P.A., Hensley, S., Joughin, I.R., Li, F.K., Madsen, S.N., Rodriguez, E. and Goldstein, R.M. 2000. Synthetic aperture radar interferometry. *Proceedings IEEE* 88: 333-382.
- Salfity, J. and Gorustovich, S.A., 1984. Paleogeografía de la cuenca del Grupo Paganzo, Paleozoico superior. *Revista de la Asociación Geológica Argentina* 38: 437-453.
- Siame, L.L. 1998. Cosmonucléide produit in-situ (^{10}Be) et quantification de la déformation active dans les Andes Centrales. Ph.D. thesis, Université de Paris-Sud, Orsay, 462 p.
- Siame, L.L., Bellier, O., Sébrier M., Boulès, D.L., Leturmy, P., Perez, M. and Araujo, M. 2002. Seismic hazard reappraisal from combined structural geology, geomorphology and cosmic ray exposure dating analyses: the Eastern Precordillera thrust system (NW-Argentina). *Geophysical Journal International* 150: 241-260.
- Siame, L.L., Bellier, O., Sébrier, M. and Araujo, M. 2005. Deformation partitioning in flat subduction setting: Case of the Andean foreland of western Argentina (28°S - 33°S). *Tectonics* (doi: 10.1029/2005TC001787): 1-24.
- Siame, L.L., Boulès, D.L., Sébrier, M., Bellier, O., Castano, J.-C., Araujo, M., Perez, M., Raisbeck, G.M. and Yiou F. 1997a. Cosmogenic dating ranging from 20 to 700 ka of a series of alluvial fan surfaces affected by the El Tigre Fault, Argentina. *Geology* 25: 975-978.
- Siame, L.L., Sébrier, M., Bellier, O., Boulès, D.L., Castano, J.-C. and Araujo, M. 1997b. Geometry, segmentation and displacement rates of the El Tigre fault, San Juan Province (Argentina) from SPOT image analysis and ^{10}Be datings. *Annales Tectonicae* 1-2: 3-26.
- Smalley, R.J., Pujol, J., Régnier, M., Chiu, J.-M., Chatelain, J.-L., Isacks, B.L., Araujo, M., and Puebla, N. 1993. Basement seismicity beneath the Andean Precordillera thin skinned thrust belt and implications for crustal and lithospheric behavior. *Tectonics* 12: 63-76.
- Smith, W.H.F. and Sandwell, D.T. 1997. Global Sea Floor Topography from Satellite Altimetry and Ship Depth Soundings. *Science* 277(5334): 1956-1962.
- Strahler, A.N. 1952. Hypsometric (area-altitude) analysis of erosional topography. *Geological Society of America, Bulletin* 63: 1117-1142.
- Zapata, T.R. and Allmendinger, R.W. 1996. Thrust-front zone of the Precordillera, Argentina: a thick-skinned triangle zone. *American Association of Petroleum Geology Bulletin* 80: 359-381.

Recibido: 30 de junio, 2006

Aceptado: 15 de noviembre, 2006